IJPSR (2021), Volume 12, Issue 1 (Research Article)

INTERNATIONAL JOURNAL OF PHARMACEUTICAL SCIENCES AND RESEARCH

Received on 01 January 2020; received in revised form, 07 April 2020; accepted, 10 April 2020; published 01 January 2021

# ANTIUROLITHIATIC ACTIVITY OF LEAF EXTRACTS OF *SYZYGIUM JAMBOS* (L.) ALSTON AND ITS ZINC NANOPARTICLES: AN *IN-VITRO* AND *IN-VIVO* APPROACH

Kangkan Deka *, Bibhuti Bhusan Kakoti and Moonjit Das

Department of Pharmaceutical Sciences, Dibrugarh University, Dibrugarh - 786004, Assam, India.

**Keywords:**

Urolithiasis, Nanoparticles, Biochemical, Histopathology

**Correspondence to Author:**
**Kangkan Deka**

Department of Pharmaceutical Sciences, Dibrugarh University, Dibrugarh - 786004, Assam, India.

**E-mail:** mailkangkan@gmail.com

**ABSTRACT:** Urolithiasis is one of the painful urologic disorders that occurs in approximately 12% of the global population. *Syzygium jambos* (L.) Alston (Family: Myrtaceae), commonly known as Rose apple in English and Bogijamun in the Assamese, is an important medicinal plant found extensively in Assam and in the Indian continent. Scientific studies confirmed that the extracts of various parts possess anticancer activity, antioxidant, analgesic, antimicrobial activities, and anti-inflammatory properties. Phytochemical and Pharmacological evaluation of the Plant was carried out with special reference to antiurolithiatic activity. The *in - vitro* evaluation was done using growth inhibition study of struvite crystals, and *in-vivo* evaluation was done by Ethylene glycol induced urolithiatic model in rats. Our investigation showed that leaf extracts and ZnO-NPs prevented the growth of urinary stones. Further studies should be done to understand pharmacological action and its possible mechanism through elaborate preclinical experimentation and clinical trials in preventing urolithiasis in susceptible populations.

**INTRODUCTION:** Urolithiasis is the formation of stone in the urinary system, *i.e.*, in the kidney, ureter, and urinary bladder or in the urethra. The term Urolithiasis is derived from 'ouron' meaning 'urine' and 'lithos', meaning 'stone' [1]. Urolithiasis, a common kidney disorder in all over the world with an estimated lifetime risk of about 2%-5% in Asia, 8%-15% in Europe and America, and around 20% in the Middle East [2]. A complex process of imbalance between promoters and inhibitors in the kidneys leads to stone formation and involves several physicochemical events commencing with crystal nucleation, aggregation, and end with retention within the urinary tract [3].

QUICK RESPONSE CODE

DOI: 10.13040/IJPSR.0975-8232.12(1).336-46

This article can be accessed online on www.ijpsr.com

DOI link: http://dx.doi.org/10.13040/IJPSR.0975-8232.12(1).336-46

The cause of urolithiasis is still unknown but probably positive family history, overweight, obesity, or increased BMI. Some other causes include low urine volume <1500 ml/day, high dietary animal protein intake, increased urine excretion of calcium oxalate, uric acid, and cystine [4]. Among the several types of kidney stones, the most common (about 80%) are calculi of calcium oxalate (CaOx) crystals existing in the form of CaOx Monohydrate (COM) and CaOx Dihydrate (COD). Calcium containing stones, especially COM (Whewellite), COD (Weddellite), and basic calcium phosphate (Apatite) happens to be in the range of 75-90%, followed by magnesium ammonium phosphate (Struvite) with a range of 10-15%, uric acid stone (3-10%) and cystine stone (0.5-1%) [5].

Extracorporeal Shock Wave Lithotripsy (ESWL) and drug among every single utilized treatment drastically changed the urological practice and

almost grow to be the standard strategy for getting rid of kidney stones; however, accompany demerits like the traumatic effects of shock waves, the persistence of residual stone fragments which may cause infection. In addition, ESWL can cause acute kidney damage, reduced renal function, hemorrhage, and high blood pressure. Thus, it is worth the effort to search for an alternative to these means by using medicinal plants or phytotherapy [6]. The extensive literature of Ayurveda states that a number of plants are useful in urinary stone treatment; most plants still have to be explored for pharmacological treatments [7].

Researches on the several plants for example *Launaea procumbens* [8], *Dolichos biflorus* [9], *Acorus calamus* L. [7], *Peperomia tetraphylla* [10], *Nigella sativa* L. [11], *Peucedanum grande* [12], *Bryophyllum pinnatum* [13], *Aerva lanata* [14], *Biophytum sensitivum* [15], *Musa paradisiaca* [16], *Bergenia ligulata* [17], *Ipomoea eriocarpa* [18] have shown promising result in the treatment of urolithiasis.

*Syzygium jambos* (L.) Alston (Family: Myrtaceae), commonly known as Rose apple in English and Bogi-jamun in the Assamese, is an important medicinal plant found extensively in the Indian continent. Scientific studies confirmed that the plant extract had anticancer activity, extracts of the rose apple leaves have antioxidant, analgesic, and anti-inflammatory properties, and the bark extracts displayed antimicrobial activities [19].

In recent years, an increased interest in the utilization of metal nanoparticles is seen due to their diverse applications in various disciplines such as medicine, biology, physics, chemistry, and material sciences [20]. Zinc oxide nanoparticles (ZnO NPs), in particular, are the perfect candidate for biological applications as they are environment friendly, non-toxic, bio-safe, and biocompatible. Moreover, the United States- Food and Drug Administration (FDA) listed ZnO and the other four zinc compounds as generally recognized as safe (GRAS) material (FDA, 2015). The ZnO NPs have been used in sunscreens, paints, and coatings as they are transparent to visible light and extremely absorbent to UV and are also used as an ingredient in antibacterial creams, ointments, and lotions, self-cleaning glass, ceramics, and deodorants [21-24].

The present study aims at evaluating the antiurolithiatic activity of leaf extracts of *Syzygium jambos* (SJ) and its Zinc oxide Nanoparticles (ZnO-NPs) both *in-vitro* as well as *in-vivo*. Single diffusion gel growth technique and Ethylene glycol-induced urolithiasis model were used to evaluate the *in-vitro* and *in-vivo* antiurolithiatic activity, respectively.

## MATERIALS AND METHODS:

**Chemicals and Reagents:** Sodium metasilicate (SMS), Ammonium Dihydrogen Phosphate (ADP), and magnesium acetate (MA), Zinc acetate, Sodium Hydroxide, Ethylene glycol, ammonium chloride, Cystone, which were procured from Sisco Research Laboratories Pvt. Ltd., and Research Lab Fine Chem Industries. Cystone was procured from Himalayan Drug Company.

**Plant:** Leaves of the plant *Syzygium jambos* (L.) Alston was collected from Dibrugarh University campus, Assam, India, in the month of August 2017. The Plant was authenticated by Dr. L. R. Saikia, Professor, Department of Life Sciences, Dibrugarh University, and a Voucher Specimen No. DULSc488 on 23/3/2018 and were preserved for future reference. Leaves were washed with water to remove dust and then shade dried. The dried leaves were then pulverized using a mechanical grinder to a coarse powder and stored in an airtight container to avoid moisture.

**Preparation of Extract:** Coarsely powdered leaves were subjected to successive extraction using the Soxhlation method. Solvents used for the extraction were in increasing order of polarity, *i.e.*, Petroleum ether (40-60°), Chloroform, Ethyl Acetate (EASJ), and Methanol (MESJ). Each extract was concentrated by distilling off the solvent in a rotary evaporator and evaporated to dryness in Petri dish on a water bath. The crude extracts were stored in a desiccator to avoid moisture.

### Biosynthesis of Zinc Oxide Nanoparticles (ZnO-NPs):

**Preparation of Aqueous Leaf Extract for the Synthesis of ZnO-NPs:** 15 g of coarsely powdered leaves were taken in 300 ml of distilled water in a 500 ml beaker, and the mixture was boiled at 60° for 10 min. The aqueous leaf extract was allowed to

cool to room temperature, filtered through Whatman no. 1 filter paper, and the filtrate was stored for further experimental use.

**Synthesis of ZnO-NPs**: To 180 ml of the above extract, 400 ml of 91 mM of zinc acetate solution (8 gm of zinc acetate was dissolved in 400 ml of distilled water) was added dropwise under continuous stirring. To the above mixture 1N NaOH was added dropwise. The reaction mixture became yellowish, and a cream-colored precipitate of zinc hydroxide was formed. The reaction mixture was left for 30 min for complete reduction to zinc hydroxide. Then the precipitate was collected by centrifugation at 10000 rpm for 10 min at 4°. The precipitate was dried at 30°. [25]

**Characterization of Biosynthesized ZnO-NPs:**

**UV–Visible Spectroscopy:** Optical density of the reaction medium was measured through UV–Vis spectroscopy of the after diluting small aliquots of reaction mixture ten times diluted with Milli-Q water and transferred to the cuvette and analysis was done using UV- 1800 SHIMADZU UV-Spectrophotometer (Kyoto, Japan), in the wavelength range of 200–600 nm. The measurement was done in order to monitor the reduction of Zinc ion.

**X-Ray Diffraction (XRD):** XRD analysis was carried out for the washed and dried sample of ZnO-NPs using Ultima IV (Rigaku, Japan) at the wavelength of 1.5406 Å. XRD was performed in the 2h range of 20–80 degrees at 40 kV and 40 mA with a divergence slit of 10 mm in 2h/h continuous scanning mode. The particle size of the formed nanoparticle was calculated by using the Debye Scherrer formula.

$$D = k\lambda/\beta \cos\theta \text{.....(Equation a)}$$

Where D is the mean size of crystallites (nm), K is crystallite shape factor a good approximation is 0.9, λ is the X-ray wavelength, β is the Full Width at Half the Maximum (FWHM) in radians of the X-ray diffraction peak, and θ is the Braggs' angle (deg.).

**Evaluation of *in-vitro* Antiurolithiatic Activity:** Struvite crystals were grown by single diffusion gel growth technique, and the growth inhibition study of the Struvite crystals was carried out in the presence of the different concentration of EASJ and MESJ and ZnO-NPs [26].

**Crystal Growth:** SMS solution having a specific gravity of 1.03 and an aqueous solution of 0.5M ADP were mixed until a pH of 7.2 was attained. About 20 ml of the gel solution was then transferred into tubes (test tubes and glassware were autoclaved at 120° for 15 min) with a length of 140mm and a diameter of 25 mm. After gelation, 10 ml of the supernatant solution of 1.0M magnesium acetate (control solution) and 1.0M magnesium acetate prepared with 0.5-2% concentrations of the leaf extracts and ZnO-NPs were gently poured on the gel. Composition and pH of the supernatant solutions are shown in **Table 1**.

**TABLE 1: COMPOSITION OF THE SUPERNATANT SOLUTION**

| Concentration | Composition | | | | | |
|---|---|---|---|---|---|---|
| | Distilled water (ml) | Magnesium Acetate (g) | EASJ (g) | MESJ (g) | ZnO-NPs (g) | pH |
| No Inhibitor | 10 | 2.144 | - | - | - | - |
| 0.5% | 10 | 2.144 | 0.050 | 0.050 | 0.050 | 7.1 |
| 1.0% | 10 | 2.144 | 0.100 | 0.100 | 0.100 | 6.5 |
| 2.0% | 10 | 2.144 | 0.200 | 0.200 | 0.200 | 6.7 |

After pouring the supernatant solution, the test tubes were capped with air-tight stoppers. In order to avoid microbial contamination, the entire procedure was carried out in an aseptic condition at room temperature in laminar airflow.

It was anticipated for the following reaction to occur between the two reactants in the gel:

$$NH_4H_2PO_4 \cdot 2H_2O + (CH_3COO)2Mg \cdot 4H_2O \rightarrow NH_4MgPO_4 \cdot 6H_2O + 2CH_3COOH$$

The apparent lengths of the growing/dissolving crystals in each of the test tubes were measured at regular intervals with the help of a traveling microscope of least count 0.001 cm. The mean length of the crystals, as well as single-factor analysis of variance (ANOVA), were calculated. The percentage inhibitions of the samples were also calculated for each day of observation. The total mass of struvite crystals in each test tube was

measured after the removal of crystals, and the yield per test tube of the crystals was obtained.

**Characterization Techniques:** Fourier transforms infrared (FTIR) spectrum was recorded and interpreted using BRUKER ALPHA-T FT-IR Spectrometer (Billerica, US).

**Statistical Analysis:** Data are expressed as mean ± standard deviation (SD) from three separate observations. Statistical analysis of the difference between groups was evaluated by one-way ANOVA followed by Dunnett's multiple comparison test using GraphPad Prism 5 software. Level of significance *P* was considered at <0.0001.

**Evaluation of *in-vivo* Antiurolithiatic Activity:** Based on the data obtained from the *in vitro* studies, the *in-vivo* antiurolithiatic study was carried out using methanolic leaf extract (MESJ) and Zinc Oxide Nanoparticles (ZnO-NPs) of aqueous leaf extract of *Syzygium jambos* (L.) Alston in male wistar rats. The ethylene glycol-induced urolithiasis model was used for the study.[18] Necessary permission in regards to the animals was obtained prior to the study from the IAEC of Dibrugarh University (Approval no. IAEC/DU 167 dtd. 12.06.2018).

**Animals:** The study was carried out with adult male Wistar rats weighing 90-140 gm. Animals were acclimatized to experimental conditions in cases and kept under standard environmental conditions (22 ± 3°; 12/12 h light/dark cycle). Water and grains were provided to all rats.

**Ethylene Glycol-Induced Urolithiasis:** All the 25 rats were divided in 5 separate groups with 5 animals in each group. Group I was taken as the control regimen, and regular food and drinking water were provided. Group II–V were given stone inducing treatment till 28th day, comprising of 1% ethylene glycol (w/v) with 1% ammonium chloride (w/v) for 4 days, followed by 1% ethylene glycol alone in the water. Group II (Disease control) received only stone-inducing treatment till the 28$^{th}$ day. Group III served as the standard control group and received antiurolithiatic drug, Cystone (500 mg/kg), from the 15$^{th}$ day till the 28$^{th}$ day. Group IV and V served as a curative regimen. Group IV received MESJ (250 mg/kg b.w.) from 1$^{st}$ day till 28$^{th}$ day, and Group V received ZnO-NPs (50 mg/kg b.w.) from 15$^{th}$ day till 28$^{th}$ day.

**Measurement of Body Weight and Water Intake:** Bodyweight (%) and water intake (24 h) were found out at the end of the 28$^{th}$ day for each group.

**Biochemical Analysis:**

**Collection and Analysis of Urine:** Urine samples (24 h) have been accumulated with the aid of keeping the rats in metabolic cages. During the urine collection period, animals were provided with free access to drinking water. Urine samples were investigated for phosphorus, calcium, and magnesium.

**Serum Analysis:** Subsequent to sacrificing of the animals, blood was collected from the rats of each group, and serum was isolated by centrifugation at 6000 rpm for 15 min and investigated for phosphorus, calcium, urea, and creatinine.

**Kidney Histopathology:** Kidneys were isolated from animals of all 5 groups and were kept in 10% formalin solution to prevent the tissues from decaying. Sections were cut with 5 µm thickness followed by its mounting on slides subsequent to staining with hematoxylin and eosin. The slides were examined under a light microscope to observe kidney architecture and CaOx deposits.

**Statistical Analysis:** Results were expressed in terms of mean ± standard error mean. Differences among data were determined using a one-way ANOVA test followed by Dunnett's multiple comparison test (GraphPad Software, Inc., version 5, CA, USA.), and *P*<0.05 was considered statistically significant.

## RESULTS:

**Characterization of ZnO-NPs:**

**UV-vis Spectroscopy**: The formation and stability of the synthesized ZnO-NPs were checked by means of observing the UV–vis absorption spectra. **Fig. 1** represents the UV-visible spectra of freshly prepared ZnO-NPs. Peak obtained at 355 nm clearly demonstrates the presence of ZnO-NPs in the reaction mixture. This result correlates with the already reported results, in which the absorption peak was found at 360 nm [27].

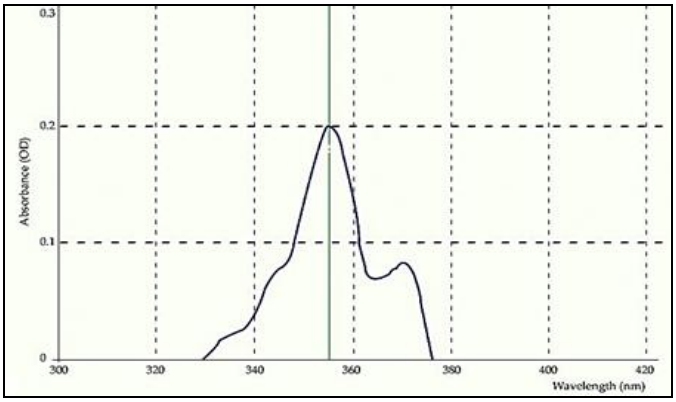


**FIG. 1: UV–VIS ABSORPTION SPECTRA OF BIOSYNTHESIZED ZnO NPs**

**X-ray Diffraction:** The XRD pattern of the ZnO-NPs **Fig. 2** matches with the standard Joint Committee on Powder Diffraction Standards (JCPDS) ZnO pattern (96-230-0451). Six sharp peaks are observed at 2θ values of31.88, 34.56, 36.41, 46.64, 56.6, and 62.9, which are indexed as (100), (002), (101), (012), (110), and (013) bands of hexagonal structures of ZnO-NPs. Using Debye Scherrer formula (Equation a), the average crystallite size of ZnO-NPs was found to be about 20 nm.

The above-obtained data matches that of the data generated by approaches carried out by Kumar *et al*. 2017,[20] Bala *et al*., 2015, [27] Geetha *et al*. 2016,[28] which thus indicates that the applied procedure for the green synthesis of ZnO-NPs was successful in accomplishing the desired nanoparticle synthesis.

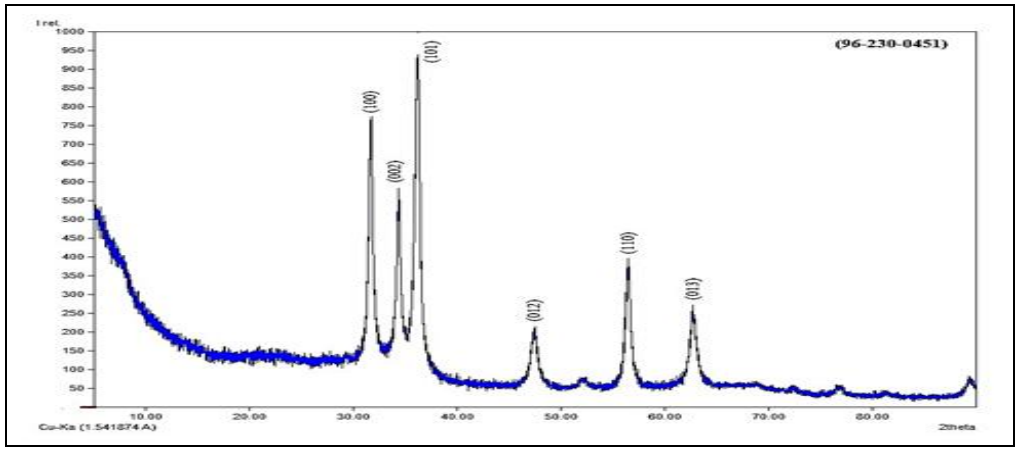


**FIG. 2: XRD PATTERN SPECTRA OF BIOSYNTHESIZED ZnO NPs**

***In-vitro* Antiurolithiatic Activity:**

**Crystal Growth and Morphologies:** Struvite crystals with two morphological shapes, namely needle type, X-shaped dendritic type, were formed in the gel. **Fig. 3** shows the struvite crystals in the gel medium with and without leaf extract solutions. **Fig. 4** shows the different types of the morphology of the gel-grown struvite crystals.

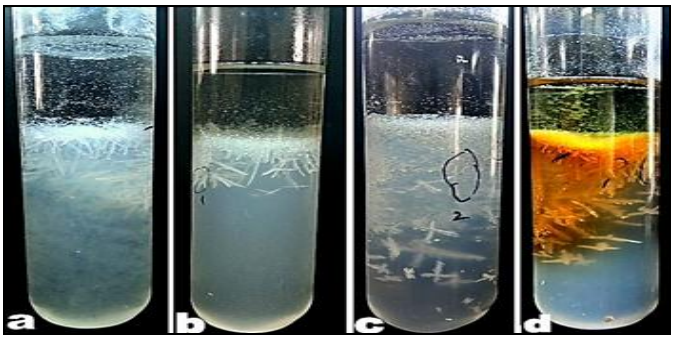


**FIG. 3: STRUVITE CRYSTALS GROWN IN THE GEL MEDIUM: (A) NO INHIBITOR (CONTROL); (B) 0.5%; (C) 1%; (D) 2%**

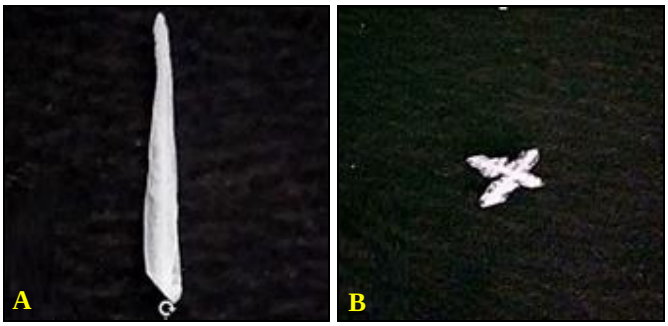


**FIG. 4: DIFFERENT TYPES OF MORPHOLOGY OF THE GEL-GROWN STRUVITE CRYSTALS. (A) NEEDLE, (B) X-SHAPED DENDRITIC**

**FTIR:** The FTIR analysis of the struvite crystals carried out between 400 and 4,000 $cm^{-1}$ was in agreement with the reported spectra. **Fig. 5** represents the spectra of gel-grown struvite crystals. The experimental and reported data of the vibrational bands are summarized below. There are four regions in the FTIR that occurred due to the various vibrations of water of crystallization, $NH_4^+$

units, tetrahedral $PO_4^{3-}$ units and metal-oxygen bonds. The absorption bands shown because of water of crystallization closely matches with the previously established peaks in several inorganic hydrated compounds [26, 31-32]. Tetrahedral $NH_4^+$ has four vibrational modes, and all the four appeared in the FTIR spectra because of its general position in the struvite crystals [26, 32, 33]. The vibrational modes of tetrahedral $PO_4^{3-}$ anions also matched the reported values [34, 35].

Observed FTIR ($cm^{-1}$) frequencies: 2919.20 (N-H stretch, $NH_4^+$ ion), 2854.35 (C-H stretch, $CH_3$), 2391.82 (H-O-H stretch, Water cluster), 1625.01 (H-O-H bend, Water cluster), 1457.57, 1375.32 (C-H bend, $CH_3$), 1259.64 (C-O stretch, Carboxylic acid), 976.65 ($PO_4^{3-}$ symmetric stretch), 800.68 (C-C stretch).

Reference FTIR ($cm^{-1}$) frequencies: 2000-3000 (N-H stretch, $NH_4^+$ ion), 2850-3000 (C-H stretch, $CH_3$), 2060-2460 (H-O-H stretch, Water cluster), 1590-1650 (H-O-H bend, Water cluster), 1375-1460 (C-H bend, CH3), 1000-1300 (C-O stretch, Carboxylic acid), 930-995 ($PO_4^{3-}$ symmetric stretch), 800-1000 (C-C stretch).

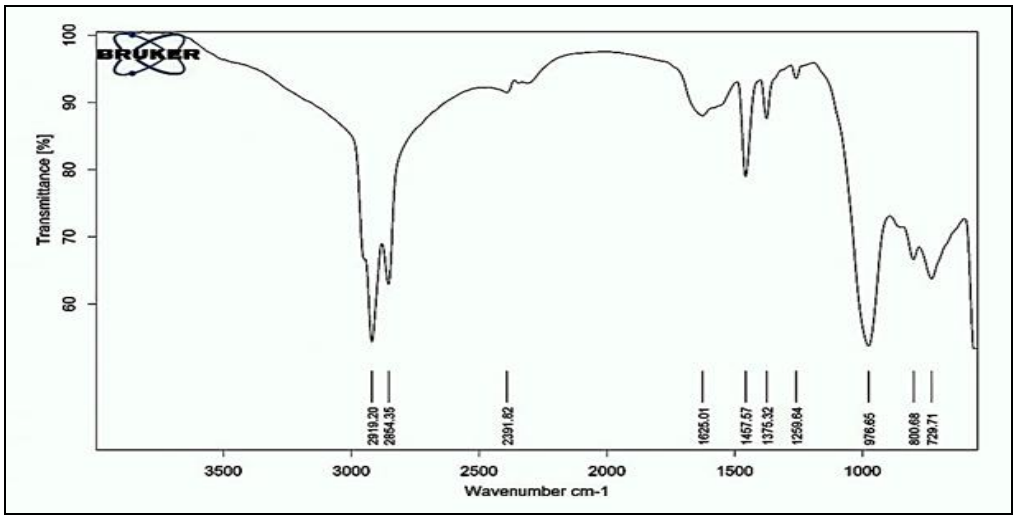


**FIG. 5: FOURIER TRANSFORM INFRARED SPECTRUM OF THE GEL-GROWN STRUVITE CRYSTALS**

**Growth-Inhibition Study:** It was observed that as the concentration of the EASJ, MESJ, and ZnO-NPs increased, the average size of the struvite crystals in the hydrogel medium decreased, as shown in **Table 2**. The average length of the struvite crystals without inhibitor was 1.243 ± 0.092 cm, but was reduced to 0.866 ± 0.060, 0.668 ± 0.050 and 0.581 ± 0.048 cm at 0.5, 1 and 2% of the EASJ respectively and for MESJ it was 0.890 ± 0.096, 0.703 ± 0.077 and 0.654 ± 0.088 cm for 0.5,1 and 2% respectively. Similarly for ZnO-NPs reduction in crystal growth was 0.833 ± 0.101, 0.711 ± 0.094 and 0.606 ± 0.106 cm for 0.5, 1.0 and 2.0% respectively. From the ANOVA single factor analysis, the differences in average length were highly significant at $P<0.0001$.

**TABLE 2: GROWTH OF STRUVITE CRYSTALS IN THE GEL FOR DIFFERENT CONCENTRATIONS OF EASJ, MESJ AND ZNO-NPs**

| Time (h) | Control | EASJ 0.5*** | EASJ 1.0*** | EASJ 2.0*** | MESJ 0.5*** | MESJ 1.0*** | MESJ 2.0*** | ZnO NP 0.5*** | ZnO NP 1.0*** | ZnO NP 2.0*** |
|---|---|---|---|---|---|---|---|---|---|---|
| 24 | 1.104 ±0.32▲ | 0.952 ±0.32 | 0.742 ±0.51 | 0.652 ±0.33 | 1.021 ±0.44 | 0.810 ±0.21 | 0.772 ±0.55 | 0.984 ±0.37 | 0.852 ±0.54 | 1.032 ±0.21 |
| 48 | 1.215 ±0.28 | 0.892 ±0.19 | 0.689 ±0.26 | 0.602 ±0.41 | 0.936 ±0.53 | 0.737 ±0.60 | 0.689 ±0.61 | 0.883 ±0.22 | 0.753 ±0.29 | 0.896 ±0.35 |
| 72 | 1.255 ±0.51 | 0.865 ±0.54 | 0.664 ±0.41 | 0.577 ±0.25 | 0.891 ±0.18 | 0.707 ±0.38 | 0.662 ±0.15 | 0.801 ±0.58 | 0.687 ±0.23 | 0.791 ±0.44 |
| 96 | 1.289 ±0.26 | 0.824 ±0.29 | 0.638 ±0.36 | 0.552 ±0.55 | 0.835 ±0.34 | 0.656 ±0.13 | 0.611 ±0.31 | 0.765 ±0.22 | 0.654 ±0.36 | 0.729 ±0.16 |
| 120 | 1.352 ±0.16 | 0.797 ±0.35 | 0.611 ±0.22 | 0.524 ±0.47 | 0.769 ±0.22 | 0.606 ±0.29 | 0.536 ±0.44 | 0.732 ±0.35 | 0.611 ±0.54 | 0.668 ±0.23 |

Note: Level of significance: ***$P<0.0001$ (one-way analysis of variance). ▲ Each value represents mean ± SD ($n = 3$).

Percentage inhibition of the struvite crystals by the EASJ, MESJ, and ZnO-NPs was studied from the second day onward, and the results are summarized in **Table 3**. In the case of EASJ the maximum inhibition of 19.63% was observed with 2% extract after the fifth day, while the minimum 16.28% inhibition was observed at 0.5% extract after the fifth day; in case of MESJ the maximum inhibition of 30.56% was observed with 2% extract after the fifth day, while the minimum 24.68% inhibition was observed at 0.5% extract after the fifth day. Similarly, in the case of ZnO-NPs the maximum inhibition of 35.27% was observed with 2% extract after the fifth day, while the minimum 25.60% inhibition was observed at 0.5% extract after the fifth day. It was concluded that the percentage inhibition increased at higher concentrations of EASJ, MESJ, and ZnO-NPs.

**TABLE 3: PERCENTAGE INHIBITION OF THE STRUVITE CRYSTALS IN DIFFERENT CONCENTRATION OF EASJ, MESJ AND ZnO-NPs**

| Day | Percentage Inhibition | | | | | | | | |
|---|---|---|---|---|---|---|---|---|---|
| | EASJ 0.5 | EASJ 1.0 | EASJ 2.0 | MESJ 0.5 | MESJ 1.0 | MESJ 2.0 | ZnO NP 0.5 | ZnO NP 1.0 | ZnO NP 2.0 |
| 2 | 6.30 | 7.14 | 7.66 | 8.32 | 9.01 | 10.75 | 10.26 | 11.61 | 13.17 |
| 3 | 9.13 | 10.51 | 11.50 | 12.73 | 12.71 | 14.24 | 18.59 | 19.36 | 23.35 |
| 4 | 13.44 | 14.01 | 15.33 | 18.21 | 19.01 | 20.85 | 22.25 | 23.24 | 29.36 |
| 5 | 16.28 | 17.65 | 19.63 | 24.68 | 25.18 | 30.56 | 25.60 | 28.29 | 35.27 |

After the growth study, struvite crystals were removed from the gel, and the total mass of the crystals for each concentration was measured. The results are summarized in **Table 4**. It was observed that the total mass of the crystals decreased with an increase in the concentration of the leaf extract.

**TABLE 4: TOTAL MASS OF THE GROWN STRUVITE CRYSTALS IN DIFFERENT CONCENTRATIONS OF EASJ, MESJ AND ZnO-NPs**

| Conc. | Control | EASJ 0.5 | EASJ 1.0 | EASJ 2.0 | MESJ 0.5 | MESJ 1.0 | MESJ 2.0 | ZnO NP 0.5 | ZnO NP 1.0 | ZnO NP 2.0 |
|---|---|---|---|---|---|---|---|---|---|---|
| Weight (g) | 1.412 ±1.02▲ | 1.315 ±0.99 | 1.224 ±0.95 | 1.091 ±1.19 | 1.230 ±0.92 | 1.152 ±0.89 | 1.043 ±1.16 | 1.215 ±0.96 | 1.163 ±1.15 | 1.072 ±0.91 |

▲Each value represents mean ± SD ($n$ = 3)

***In-vivo* Antiurolithiatic Activity:**

**Measurement of Body Weight and Water Intake:** Bodyweight and water intake that were recorded before the beginning of treatment were practically the same for all the groups. **Table 5** represents the parameters recorded after the treatment. Loss in body weight of the animals was observed in the stone-induced group ($P$<0.001 *vs*. Group I), whereas the other group animals showed a significant gain in their body weights after the experiment. There occurred no such noteworthy change in the water intake among the groups except in the stone-induced group, which showed significantly high as compared to the control group ($P$ < 0.001 *vs*. Group I).

**Biochemical Analysis:**

**Urine Analysis: Table 5** shows the urine concentration of phosphorus, calcium, and magnesium present in Group I–V. Administration of 1% ethylene glycol in drinking water to the male Wistar rats caused a significant ($P$< 0.001 *vs*. Group I) increase of phosphorus and calcium concentration and a decrease in the magnesium concentration in urine of the stone-induced group (Group II). However, treatment with MESJ (250mg/kg b.w.) and ZnO-NPs caused notable ($P$<0.001 *vs*. Group II) diminution in the phosphorus and calcium excretion and increased the magnesium excretion in urine in both the groups (Group IV and V, respectively) and were comparable to the standard group (Group III, cystone-treated).

**Serum Analysis:** Renal function was assessed by estimating serum phosphorus, calcium, urea, and creatinine in Group I–V **Table 5**. The concentration of phosphorus, calcium, urea, and creatinine in the serum was significantly ($P$< 0.001 *vs*. Group I) increased in the stone-induced group, indicating renal harm/damage. However, treatment with MESJ (250mg/kg b.w.) and ZnO-NPs significantly ($P$< 0.001 vs. Group II) reduced the concentrations of phosphorus, calcium, urea, and creatinine in the

serum in both the groups to a close to a normal level and were comparable to the standard group.

**Kidney Histopathology:** Kidney histopathological examination revealed no CaOx crystal deposit or other abnormalities in the kidney of the control group (Group I), as shown in **Fig. 6a**. On the other hand, many CaOx crystal deposits in the renal tubules and congestion and dilation of the parenchymal blood vessels were seen in the renal tissue of the stone-induced group (Group II) as shown in **Fig. 6b**. In the standard group (Group III), the kidney showed normal architecture with dilation of tubules in the corticomedullary junction, minima interstitial inflammation, and occasional renal tubules showed CaOx crystal deposits **Fig. 6c**. In MESJ (Group IV) and ZnO-NPs (Group V) groups, the kidney showed normal architecture, less tissue damage, and occasional renal tubules showed CaOx crystal deposit **Fig. 6d** and **6e**.

**TABLE 5: EFFECT OF *SYZYGIUM JAMBOS* ON PARAMETERS IN UROLITHIATIC MALE WISTAR RATS**

| Parameter (unit) | Group I (control) | Group II (stone-induced) | Group III (standard) | Group IV (MESJ) | Group V (ZnO NP) |
|---|---|---|---|---|---|
| Change in body weight (%) | 36.4±0.98 | -32..62±1.02*$^{a}$ | 16.5±2.02*$^{a}$*$^{b}$ | -10.5±2.61*$^{a}$*$^{b}$ | -2.3±1.36*$^{a}$*$^{b}$ |
| Water intake (ml/24 h) | 7.2±1.12 | 13.5±0.76*$^{a}$ | 9.7±1.56$^{▲a}$■$^{b}$ | 11.3±1.03*$^{a}$$^{▲b}$ | 10.5±0.91$^{ɪa}$$^{ɪb}$ |
| **URINE (mg/dl)** | | | | | |
| Phosphorus | 7.2±3.54 | 13.3±3.04*$^{a}$ | 10.4±2.15$^{ɪa}$$^{ɪb}$ | 11.5±1.35*$^{a}$$^{▲b}$ | 11.1±1.02■$^{a}$$^{▲b}$ |
| Calcium | 8.4±2.68 | 14.5±2.01*$^{a}$ | 11.3±0.82$^{ɪa}$$^{ɪb}$ | 12.8±0.68*$^{a}$$^{▲b}$ | 12.2±0.82■$^{a}$$^{▲b}$ |
| Magnesium | 6.7±1.65 | 1.5±0.86*$^{a}$ | 2.6±3.04*$^{a}$$^{▲b}$ | 4.2±2.15$^{▲a}$$^{▲b}$ | 3.1±0.79■$^{a}$$^{▲b}$ |
| **SERUM (mg/dl)** | | | | | |
| Phosphorus | 9.1±1.03 | 15.8±3.56*$^{a}$ | 11.3±0.95$^{▲a}$*b | 12.7±1.32■$^{a}$$^{ɪb}$ | 11.9±0.84$^{▲a}$■$^{b}$ |
| Calcium | 8.8±0.85 | 14.9±0.76*$^{a}$ | 11.6±1.15$^{▲a}$$^{ɪb}$ | 12.9±0.92*$^{a}$$^{▲b}$ | 12.1±1.26$^{ɪa}$$^{▲b}$ |
| Urea | 14.5±0.32 | 27.9±0.56*$^{a}$ | 17.2±0.68$^{▲a}$*$^{b}$ | 19.4±0.84*$^{a}$*$^{b}$ | 18.3±1.03■$^{a}$*$^{b}$ |
| Creatinine | 0.4±1.15 | 1.29±2.16$^{▲a}$ | 0.91±0.92$^{▲a}$$^{▲b}$ | 1.05±1.24$^{▲a}$$^{▲b}$ | 0.98±2.10$^{▲a}$$^{▲b}$ |

Values for urine parameters are measured in 24 h urine sample. All values are stated as mean ± SD ($n$=5). $^{a}$Comparisons are made with Group I, $^{b}$Comparisons are made with Group II,*$P$<0.001 $^{▲}$ns ■$P$<0.01$^{ɪ}$P < 0.05, SD= Standard Deviation

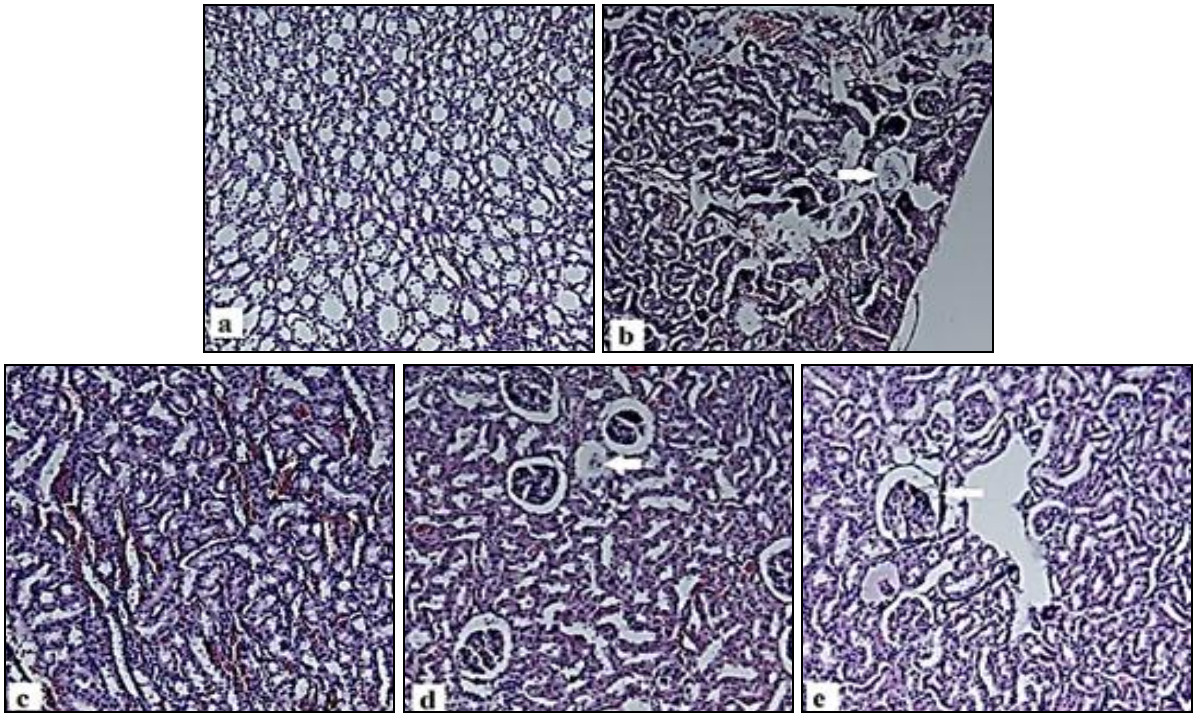


**FIG. 6: KIDNEY HISTOPATHOLOGY (A) GROUP I (CONTROL) (B) GROUP II (STONE INDUCED) (C) GROUP III (STANDARD) (D) GROUP IV (MESJ) (E) GROUP V (ZnO NP).** *White arrow is to indicate stone

**DISCUSSION**: For the evaluation of the *in-vitro* antiurolithiatic activity, struvite crystals were grown by using a single gel diffusion technique, and the growth inhibition of the struvite crystals in the presence of EASJ, MESJ, and ZnO NP were studied. It was observed that as the concentration of

the EASJ, MESJ, and ZnO-NPs increased, the average size of the struvite crystals in the hydrogel medium decreased. From the growth inhibition of struvite crystals by EASJ, MESJ, and ZnO NP, two-stage inhibition hypothesis can be recommended. They are expected to inhibit the growing struvite crystals in two different stages: (i) by forming stable complexes with $Mg^{2+}$ ion and therefore clogging the availability of $Mg^{2+}$ ions for the growth of struvite crystals and (ii) by adsorption on the growing crystalline surface. A large amount of adsorption of an organic compound may induce desorption of complex formed by $Mg^{2+}$ ions, thereby weakening the bonds of crystals resulting in fragmentation.

For the evaluation of *in vivo* antiurolithiatic activity, male Wistar rats were chosen to induce urolithiasis with 1% ethylene glycol (w/v) with 1% ammonium chloride (w/v). Likewise, to that of the previously reported studies, the present experiment also showed significant elevation in the concentration of phosphorus (hyperphosphaturia) and calcium (hypercalciuria) and lowered concentration of magnesium (hypomagnesemia) in the urine of the stone-induced group **Table 5** [36, 37]. The increased calcium may have occurred due to excessive tubular damage in the kidney prompting excretion of intracellular calcium *via* urine. Hypercalciuria leads to elevated phosphorus leakage. Elevated urinary phosphorus excretion along with oxalate stress appears to offer suitable surroundings for stone formation with the aid of forming calcium phosphate crystals, which epitaxially causes CaOx deposition [36]. Magnesium is considered as a potent inhibitor of CaOx crystals because it causes a decrease in supersaturation [18, 36].

In the stone-induced group, there was a substantial increase in phosphorus levels compared to the control group. The magnesium level was essentially diminished in the stone-induced group as compared to the control group, due to supersaturation and metabolic acidosis. However, during the administration of MESJ and ZnO-NPs, the calcium and phosphorus level diminished to a near-normal level, and magnesium excretion was restored in Group IV and V compared to the stone-induced group, which demonstrates that MESJ and ZnO-NPs are effective in inhibiting hypercalciuria, hyperphosphaturia, and hypo-magnesemia.

In urolithiasis, the stones in the urinary tract obstruct urine outflow bringing about the reduced glomerular filtration rate. This leads to the deposition of waste products in the blood, specifically nitrogenous substances, for example, urea and creatinine [6, 7]. Accordingly, in the present test, serum concentrations of phosphorus, calcium, urea, and creatinine were determined. As shown in **Table 5**, the phosphorus, calcium, urea, and creatinine levels in the stone-induced group were higher than the control group. However, treatment with MESJ and ZnO-NPs significantly reduced the phosphorus, calcium, urea, and creatinine levels. Our results are compatible with the previous findings. In the stone-induced group, the high level of these parameters was because of the CaOx stone formation in the urinary tract, which led to the deposition of waste products in the blood. However, treatments with MESJ and ZnO-NPs inhibited the stone formation and brought down these parameters.

**CONCLUSION:** The present investigation showed that MESJ and ZnO-NPs *Syzygium jambos* prevented the growth of urinary stones. Further studies should be done to understand pharmacological action and its possible mechanism through elaborate preclinical experimentation and clinical trials in preventing urolithiasis in the susceptible population.

**ACKNOWLEDGEMENT:** Authors deeply acknowledge the facilities provided by Dibrugarh University in terms of library and experimental facilities.

**CONFLICTS OF INTEREST:** The authors declare no conflict of interest.

**REFERENCES:**

1. Vijaya T, Kumar MS, Chalapathi NVR, Babu AN, Ramarao N and Ramarao NV: Urolithiasis and its causes-short review. The Journal of Phytopharmacology 2013; 2(3): 1-6.
2. Nizami AN, Rahman A, Ahmed NU and Islam S: Whole Leea macrophylla ethanolic extract normalizes kidney deposits and recovers renal impairments in an ethylene glycol-induced urolithiasis model of rats. Asian Pacific Journal of Tropical Medicine 2012; 5(7): 533-38.
3. Jagannath N, Chikkannasetty SS, Govindadas D and Devasankaraiah G: Study of antiurolithiatic Activity of

Asparagus racemosus on albino rats. Indian Journal of Pharmacology 2017; 44(5): 576-79.
4. Vyas N and Argal A: Antiurolithiatic Activity of extract and oleanolic acid isolated from the roots of Lantana camara on Zinc Disc Implantation Induced Urolithiasis. ISRN Pharmacology 2013; 951795.
5. Sasikala V, Ramu S and Vijayakumari: *In-vitro* evaluation of *Rotula aquatica* Lour. for antiurolithiatic activity. Journal of Pharmacy Research 2013; 6(3): 378-82.
6. Bouanani S, Henchiri C, Migianu-Griffoni E, Aouf N and Lecouvey M: Pharmacological and toxicological effects of *Paronychia argentea* in experimental calcium oxalate nephrolithiasis in rats. Journal of Ethnopharmacology 2010; 129(1): 38-45.
7. Ghelani H, Chapala M and Jadav P: Diuretic and antiurolithiatic activities of an ethanolic extract of *Acorus calamus* L. rhizome in experimental animal models. Journal of Traditional and Complementary Medicine 2016; 6(4): 431-36.
8. Makasana A, Ranpariya V, Desai D and Mendpara J: Evaluation for the anti-urolithiatic Activity of *Launaea procumbens* against ethylene glycol-induced renal calculi in rats. Toxicology Reports 2014; 1: 46-52.
9. Saha S, Verma RJ, Saha S and Verma RJ: Antinephrolithiatic and antioxidative efficacy of *Dolichos biflorus* seeds in a lithiasis rat model. Pharmaceutical Biology 2015; 53(1): 16-30.
10. Nishanthi M, Vijayakumar B and Aanandhi MV: Antiurolithiatic activity of the plant extracts of *Peperomia tetraphylla* on ethylene glycol induced urolithiasis in rats. Rasaya J Chem 2016; 9(2): 294-99.
11. Benhelima A, Kaid-Omar Z, Hemida H and Ibn A: Nephroprotective and diuretic effect of Nigella sativa L seeds oil on lithiasic. African Journal of Traditional, Complementary and Alternative Medicine 2016; 13(6): 204-14.
12. Ajij S, Makbul A and Husain S: Antilithiatic effect of *Peucedanum grande* C. B. Clarke in chemically induced urolithiasis in rats. Journal of Ethnopharmacology 2016; 194(4): 1122-29.
13. Yadav M, Gulkari VD and Wanjari MM: *Bryophyllum pinnatum* leaf extracts prevent formation of renal calculi in lithiatic rats. Ancient Science of Life 2018; 36(2): 90-97.
14. Dinnimath BM, Jalalpure SS and Patil UK: Antiurolithiatic activity of natural constituents isolated from Aerva lanata. Journal of Ayurveda and Integrative Medicine 2017; 8(4): 226-32.
15. Pawar AT and Vyawahare NS: Protective effect of ethyl acetate fraction of *Biophytum sensitivum* extract against sodium oxalate-induced urolithiasis in rats. Journal of Traditional and Complementary Medicine 2017; 7(4): 476-86.
16. Panigrahi PN, Dey S, Sahoo M and Dan A: Antiurolithiatic and antioxidant efficacy of *Musa paradisiaca* pseudostem on ethylene glycol-induced nephrolithiasis in rat. Indian Journal of Pharmacology 2018; 49(1): 77-83.
17. Sharma I, Khan W, Parveen R, Alam J, Ahmad I, Hafizur M and Ahmad S: Antiurolithiasis activity of bioactivity guided fraction of *Bergenia ligulata* against ethylene glycol induced renal calculi in rat. BioMed Research International 2017; 1-10.
18. Das M and Malipeddi H: Antiurolithiatic Activity of ethanol leaf extract of *Ipomoea eriocarpa* against ethylene glycol-induced urolithiasis in male Wistar rats. Indian Journal of Pharmacology 2016; 48(3): 270-74.
19. Lim TK: Edible Medicinal And Non-Medicinal Plants: Fruits, Springer Science + Business Media B.V. 2012; 3: 760-66.
20. Chaudhuri SK and Malodia L: Biosynthesis of zinc oxide nanoparticles using leaf extract of *Calotropis gigantea*: characterization and its evaluation on tree seedling growth in nursery stage. Appl Nanosci. Springer Berlin Heidelberg 2017; 7(8): 501-12.
21. Vaseem M, Umar A and Hahn Y: ZnO nanoparticles: growth, properties and applications. Metal Oxide Nanostructures and Their Applications 2010; 5: 1-36.
22. Rosi NL and Mirkin CA: Nanostructures in biodiagnostics. Chemical Reviews 2005; 105(4): 1546-62.
23. Franklin NM, Rogers NJ, Apte SC, Batley GE, Gadd GE and Casey PS: Comparative toxicity of nanoparticulate ZnO, bulk ZnO and $ZnCl_2$ to a freshwater microalga (*Pseudokirchneriella subcapitata*): the importance of particle solubility. Environmental Science and Technology 2006; 41(24): 8484-90.
24. Azam A, Ahmed AS, Oves M, Khan MS, Habib SS and Memic A: Antimicrobial Activity of metal oxide nanoparticles against Gram-positive and Gram-negative bacteria: A comparative study. International Journal of Nanomedicine 2011; 6: 6003-09.
25. Bala N, Saha S, Chakraborty M, Maiti M, Das S, Basu R and Nandy P: Green synthesis of zinc oxide nanoparticles using *H. subdariffa* leaf extract: Effect of temperature on synthesis, anti-bacterial and anti-diabetic activity. Royal Society of Chemistry Advances 2015; 5: 4993-5003.
26. Das M, Malipeddi H, Nambiraj NA and Rajan R: Phytochemical analysis, antioxidant activity and *in-vitro* growth inhibition of struvite crystals by *Ipomoea eriocarpa* leaf extracts. Journal of Food Biochemistry 2016; 40(2): 148-60.
27. Jayarambabu N, Sivakumari B and Prabhu YT: Germination and growth characteristics of mungbean seeds affected by synthesized zinc oxide nanoparticles. International Journal of Current Engineering and Technology 2014; 4(5): 3411-16.
28. Geetha MS, Nagabhushana H and Shivananjaiah HN: Green mediated synthesis and characterization of ZnO nanoparticles using *Euphorbia jatropa* latex as reducing agent. Journal of Science : Advanced Materials and Devices 2016; 1(3): 301-10.
29. Miller FA and Wilkins CH: Infrared spectra and characteristic frequencies of inorganic ions. Analytical Chemistry 1952; 24: 1253-94.
30. Lucchesi PJ and Glasson WA: Infrared investigation of bound water in hydrates. J Am Chem Soc 1956; 78: 1347-48.
31. Gamo I: Infrared spectra of water of crystallization in some inorganic chlorides and sulfates. Bull Chem Soc Jpn 1961; 34: 760-64.
32. Chauhan CK and Joshi MJ: *In-vitro* crystallization, characterization and growth-inhibition study of urinary type struvite crystals. Journal of Crystal Growth 2013; 362: 330-7.
33. Shashikala MN, Elizabeth S, Chary BR and Bhat H: Raman and infrared spectroscopic studies of the new ferroelectric crystal telluric acid ammonium phosphate. Current Science 1987; 56(17): 861-63.
34. Frost RL, Weier ML, Martens WN, Henry DA and Mills SJ: Raman spectroscopy of newberyite, hannayite and struvite. Spectrochimica Acta Part A 2005; 62: 181-88.
35. Khalil SKH, Azooz MA and Division P: Application of vibrational spectroscopy in identification of the

composition of the urinary stones. Journal of Applied Sciences Research 2007; 3(5): 387-91.

36. Karadi RV, Gadge NB, Alagawadi KR and Savadi RV: Effect of *Moringa oleifera* Lam. root wood on ethylene glycol induced urolithiasis in rats. Journal of Ethnopharmacology 2006; 105: 306-11.
37. Selvam R, Kalaiselvi P, Govindaraj A, Murugan VB and Kumar ASS: Effect of *A. lanata* leaf extract and *Vediuppu chunnam* on the urinary risk factors of calcium oxalate urolithiasis during experimental hyperoxaluria. Pharmacological Research 2001; 43(1): 89-93.

**How to cite this article:**
Deka K, Kakoti BB and Das M: Antiurolithiatic activity of leaf extracts of *Syzygium jambos* (L.) alston and its zinc nanoparticles: an *in-vitro* and *in-vivo* approach. Int J Pharm Sci & Res 2021; 12(1): 336-46. doi: 10.13040/IJPSR.0975-8232.12(1).336-46.